INTERNATIONAL JOURNAL OF CLIMATOLOGY
Int. J. Climatol. (2008)
Published online in Wiley InterScience
(www.interscience.wiley.com) DOI: 10.1002/joc.1821

RMetS
Royal Meteorological Society

An analysis of present and future ECHAM5 pressure fields using a classification of circulation patterns

M. Demuzere,[a]* M. Werner,[b,d] N. P. M. van Lipzig[a] and E. Roeckner[c]

[a] *Physical and Regional Geography Research Group, K. U. Leuven, Leuven, Belgium*
[b] *Max-Planck-Institute for Biogeochemistry, Jena, Germany*
[c] *Max- Planck-Institute for Meteorology, Hamburg, Germany*
[d] *Leibniz-Association, Bonn, Germany*

ABSTRACT: Several subjective and objective methods for the classification of circulation patterns into categories have been developed over the past century. In this study, we used the automated Lamb weather type (WT) classification method, based on mean sea level pressure (MSLP) to examine present and future circulation patterns above Western and Central Europe. First, the European Center for Medium-Range Weather Forecast 40-year reanalysis data (ECMWF-ERA40) is used to evaluate the occurring WTs within the newly developed ECHAM5-MPI/OM model for the period 1961–2000. Our analysis shows that the ECHAM5 model is capable of reproducing circulation patterns for the October to April season. For the remaining part of the year, there are some significant differences in eastern and western directional circulation types. Therefore, in the second part of this study, past, present and future ECHAM5 pressure fields are investigated for the autumn and winter season only. Finally, long-term trends of MSLP fields of the A1B scenario simulation using ECHAM5-MPI/OM for the period 1860–2100 show a significant increase in western circulation and anticyclonic WTs over Western and Central Europe, accompanied by a decrease in eastern circulation and cyclonic WTs. Copyright © 2008 Royal Meteorological Society

KEY WORDS circulation types; automatic Lamb weather type classification; a coupled general circulation model diagnostic tool; synoptic climatology; NAO index

Received 16 May 2008; Revised 29 October 2008; Accepted 30 October 2008

1. Introduction

Over the past decade, scientific interest in the use of circulation patterns to describe and analyse a wide array of climatologically different situations has been steadily increasing. For example, several studies have been exerted correlating near surface meteorological variables to large-scale circulation pattern changes (Buishand and Brandsma, 1997; Trigo and Dacamara, 2000; Buchanan *et al*., 2002; Fowler and Kilsby, 2002; Post *et al*., 2002). For Western Europe and the North Atlantic sector, a major part of the formation and variability in circulation patterns is strongly influenced by the passage of high and low-pressure systems in the mid-latitudes. On the contrary, spatial and temporal changes in these patterns will lead to changes in Western European climatic conditions. Thus, it is of great interest to analyse and compare the main circulation patterns and their variability over Western Europe with other important climate indices and patterns for this region, e. g. the North Atlantic Oscillation (NAO). The NAO has been investigated extensively (Marshall *et al*. (2001) – and references herein) and it has been shown that, for the mid-latitudes, the NAO is the major winter climate mode, accounting for about one third of the inter-annual variability (Schwierz *et al*., 2006). Furthermore, the NAO has already been examined in relation to extreme intensified cyclones (Rogers, 1997; Serreze *et al*., 1997; Ulbrich and Christoph, 1999; Raible and Blender, 2004) and mean flow (Raible, 2007) or blocking-like patterns over central to northern Europe (Scherrer *et al*., 2006; Schwierz *et al*., 2006).

Analyses of circulation patterns and their variability over Western Europe can be either performed by using observational data, i. e. reanalysis data sets, or by using data sets from coupled general circulation model (CGCM) simulations. The latter will not only allow examining past and presenting situations but also enables studying potential future changes with respect to different climate scenarios. In addition, a comparison of circulation patterns imprinted in reanalysis and CGCM data sets can be used as a novel, unique method to explore the accurateness of CGCMs. However, until now only few studies have examined the strength of CGCMs in reproducing circulation patterns (Huth, 2000). Several other studies have evaluated the potential to use blocking as a diagnostic tool for climate models (e. g. Tibaldi, 1993; D'Andrea *et al*., 1998). However, the use of blocking techniques as a diagnostic tool is intrinsically limiting the research to some very specific climate features. A more

* Correspondence to: M. Demuzere, Physical and Regional Geography Research Group, K. U. Leuven, Celestijnenlaan 200E, B-3001, Heverlee, Belgium. E-mail: Matthias.Demuzere@geo.kuleuven.be

Copyright © 2008 Royal Meteorological Society

broad approach using a circulation classification method can give a much more detailed insight on a synoptic time scale, as such a method can identify not only the position of cyclones and anticyclones (cyclone detection and blocking phenomena), but also the strength and frequencies of zonal and meridional mean flow patterns and the transition between different circulation patterns.

The main focus of our study is the use of an automatic version the Lamb weather type (WT) classification method (Jenkinson and Collison, 1977; Jones *et al*., 1993; Trigo and Dacamara, 2000) as a diagnostic tool to evaluate ECHAM5 pressure fields and to study trends in the frequency of occurrence of circulation patterns for the period 1860–2100. This automatic weather type scheme grid (WT-scheme), initially developed for the British Isles, is centred above Belgium. This region is chosen because of future planned studies on the use of circulation classifications for air quality studies in Belgium. However, our method encompasses the circulation patterns for the larger Western and Central European Region and therefore, our results are of interest for this larger region.

The method was designed as an automatic version of Lamb's classification. Buishand and Brandsma, 1996; Trigo and Dacamara, 2000; Buchanan *et al*., 2002; Fowler and Kilsby, 2002 and Post *et al*., 2002 for example, describe previous studies and applications. Mostly, local meteorological station measurements are used to establish the relations between WTs and local surface characteristics, while daily gridded fields of sea level pressure (SLP) from NCEP/NCAR or European Center for Medium-Range Weather Forecast (ECMWF) reanalysis data provide the pressure input for the WT-scheme. In this study we use the European Center for Medium-Range Weather Forecast 40-year reanalysis data (ECMWF-ERA40)(Uppala *et al*., 2005) to evaluate the SLP fields from the ECHAM5-MPI/OM model.

The 1961–2000 ERA40 period is used to evaluate the ECHAM5 capabilities in generating the SLP fields. Secondly, climatological trends based on the WTs are calculated for the period 1860–2100. Finally, a comparison of changes in WTs between the A1B, B1 and A2 IPCC scenarios of the ECHAM5-MPI/OM model for the period 2000–2100 is conducted.

This paper is organized as follows. In Section 2 a brief overview is given of the data and models used in this study, thereby describing both ECMWF-ERA40 data and the general circulation model ECHAM5-MPI/OM, and the Lamb WT method used to construct a daily circulation pattern database. In Section 3 the result of the sensitivity of the Lamb WT number of unclassified days on grid size and resolution is presented, followed by a comparison of ECHAM5-MPI/OM pressure fields with ERA40 data. Hereby, also the relation between WT and NAO index and related cyclone identification and blocking features are investigated. Furthermore, climatic trends are investigated using the IPCC scenarios provided by ECHAM5-MPI/OM. Section 4 discusses our results and presents the conclusions.

2. Data and methods

2.1. Data

In this study we use the ECMWF-ERA40 SLP dataset on a 2.5 $\times$ 2.5 grid, for the larger European Atlantic Region (27.5 W–27.5 E, 85–15 N), centred above Belgium. The 6 hourly SLP values (00 h, 06 h, 12 h, 18 h) are averaged over a 24 hourly period in order to obtain daily mean sea level pressure (MSLP) fields for the period 1961–2000 (CTL_{ERA40}). The fields are averaged to seasonal and yearly means. The ECHAM5-MPI/OM SLP fields for 1961–2000 (CTL_{ECHAM5}) are generated with the coupled atmosphere-ocean model (ECHAM5/MPI-OM) at T63L31 resolution in the framework of the 4th IPCC assessment report.

The coupled model used in this study consists of new model versions for both the atmosphere and the ocean. In the atmosphere model (ECHAM5; Roeckner *et al*., 2003, 2006a) vorticity, divergence, temperature and the logarithm of surface pressure are represented by a truncated series of spherical harmonics (triangular truncation at T63), whereas the advection of water vapour, cloud liquid water and cloud ice is treated by a flux-form semi-Lagrangian scheme. A hybrid sigma/pressure system is used in the vertical direction (31 layers with the top model level at 10 hPa). The model uses state-of-the-art parameterizations for short-wave and long-wave radiation, stratiform clouds, cumulus convection, boundary layer and land surface processes, and gravity wave drag. The ocean model (MPI-OM; Marsland *et al*., 2003) uses the primitive equations for a hydrostatic Boussinesq fluid with a free surface. The vertical discretization is on 40 z-levels, and the bottom topography is resolved by means of partial grid cells. The ocean has a nominal resolution of 1.5 and the poles of the curvilinear grid are shifted to land areas over Greenland and Antarctica. Concentration and thickness of sea ice are calculated by means of a dynamic and thermodynamic sea ice model. In the coupled model (Jungclaus *et al*., 2006), the ocean passes to the atmosphere the sea surface temperature (SST), sea ice concentration, sea ice thickness, snow depth on ice, and the ocean surface velocities. The atmosphere runs with these boundary values for one coupling time step (one day) and accumulates the forcing fluxes. These fluxes are then transferred to the ocean. The model does not employ flux adjustments.

Global ECHAM5-MPI/OM SLP datasets were provided by the Max-Planck-Institute for Meteorology, Hamburg, for the years 1860–2100. The available simulations include three IPCC scenarios A1B, B1 and A2 between years 2001 and 2100 (Roeckner *et al*., 2006b), for which SLP fields are available at a 6-hourly resolution ($SCEN_{A1B-Coupled}$). Pressure data for an area identical to the selected ECMWF-ERA40 region were extracted from the T63 ECHAM5-MPI/OM SLP grid and re-gridded by conservative remapping to a 2.5 $\times$ 2.5 regular lat/lon grid, which can directly be used in the WT-scheme.

Copyright © 2008 Royal Meteorological Society

DOI: 10.1002/joc

2.2. Automatic classification method

A method to classify daily circulation patterns was originally developed by Lamb (1972). This subjective classification used surface pressure synoptic charts describing the flow in the 500-hPa level in the atmosphere. To avoid dependency of the daily WTs on experience and consistency of the researcher, this method was objectified by Jenkinson and Collison (1977). Moreover, as shown by Conway and Jones (1998), circulation patterns fundamentally control meteorological characteristics on the surface, whereby the use of SLP has a lot of advantages. Previous studies done by McKendry *et al*. (2006) show that upper pressure level patterns are less variable than surface pressure patterns and that particular upper level patterns may be associated with a large range of pressure synoptic types. Therefore the WT method uses surface pressure, which is more appropriate for the classification of circulation patterns than upper level pressure patterns. On the basis of the Lamb method, the WT circulation pattern for a given day is described using the locations of the high and low-pressure centres that determine the direction of the geostrophic flow. It uses coarsely gridded pressure data on a 16-point moveable grid and is therefore easily applicable in any area with available data.

This method allows 27 different classification of WTs to be defined, including eight main directional types: north, north-east, east, south-east, south, south-west, west, north-west and three non-directional types: anticyclonic, cyclonic and unclassified types. Sixteen hybrid types (combination of directional and non-directional types) are also recognized (Lamb, 1972). These types are characterized through the use of a set of indices associated to the direction and vorticity of geostrophic flow. The indices used are the following: southerly flow component of the geostrophic surface wind (SF), westerly flow component of the geostrophic surface wind (WF), resultant flow (FF), southerly shear vorticity (ZS), westerly shear vorticity (ZW) and total shear vorticity (Z). These indices were computed using SLP values obtained for the retained number of grid points, and are both for the flow units as for the geostrophic vorticity expressed in hPa. The WTs are defined by comparing values of FF and Z:

- Direction of flow (in degrees) is given by $\tan^{-1}$ (WF/SF), 180 being added if WF is positive. The appropriate wind direction is computed using an eight-point compass, allowing 45 per sector.
- If |Z| < FF, flow is essentially straight and considered to be of a pure directional type (eight different possibilities according to the compass directions).
- If |Z| > 2FF, the pattern is considered to be of a pure cyclonic type if $Z > 0$, or of a pure anticyclonic type if $Z < 0$.
- If FF < |Z| < 2FF, flow is considered to be of a hybrid type and is therefore characterized by both direction and circulation (16 different types).
- If Z or $FF < 6$, than a day is classified as 'unclassified'.

The latter point reveals that a threshold value for Z or FF is used to define whether a day is allocated as unclassified or not. For the analyses of the SLP fields, values of Z and FF do not show any specific clustering or grouping around a specific threshold value, which is in line with the findings of Goodess (2000). Therefore, it is not necessary to implement another more useful cut-off point for our central and Western European grid area and hence the original threshold value of 6, defined originally for a grid centred on the British Isles, was retained (Jones *et al*., 1993).

The analysis of the number of occurrences for each WT shows relatively small numbers for the sixteen hybrid groups. Moreover, differences in occurrence within one direction (including both the cyclonic and anticyclonic type) are small compared to differences between different directions of types. Therefore the 27 WTs are combined in a smaller number of main groups, this according to their directional characteristics. All types, both from the pure directional and hybrid types, with the same directional component are combined into the same directional group/type. This results in eight directional types (e.g. N(d) [directional North] = N [North], CN [cyclonic North], AN [Anticyclonic North]), two pure vorticity types A [anticyclonic] and C [cyclonic] and the U [unclassified] type, so 11 types in total (Table I). This strategy of reducing the number of classes facilitates the inter-comparison between classification types derived from both ECHAM5-MPI/OM and ECMWF-ERA40 SLP fields. Figure 1 depicts the SLP composite maps for the 11 WTs separately for the ECMWF-ERA40 SLP reference dataset.

First, the number of WTs will be derived based on ECHAM5-MPI/OM and ECMWF-ERA40 SLP fields for the period 1961–2000. To assess whether there are significant differences in observed and modelled frequency distribution averaged over all types and for different periods of time (year, season, month), the χ^2 test is applied using a 0.1 significance level (Chernoff and Lehmann, 1954). In this way, it is possible to get more insight in the overall model performance in terms of WTs over the 40-year period. Inter-annual variability for each WT individually is tested with the student t-test on a monthly time scale. To investigate whether differences in trends of WTs based on the three different IPCC scenarios are significant, the Mann-Kendall test (e.g. Verstraeten *et al*., 2006) was used, using a statistical significance of 10%.

3. Results

3.1. Grid sensitivity of the WT-scheme

Previous studies using the WT classification scheme used the 16-grid points configuration with a 5 grid resolution (Buishand and Brandsma, 1996; Trigo and Dacamara, 2000; Fowler and Kilsby, 2002; Post *et al*., 2002 and Buchanan *et al*., 2002). One would expect that grid size and resolution play an important role in the

Copyright © 2008 Royal Meteorological Society

DOI: 10.1002/joc

Table I. Overview of the weather types, representing the 26 + 1 JC weather types and the reduced eight directional weather type groups (right column).

Pure Types	Directional Types	Hybrid Types		
U	N	CN	AN	N(d)
C	NE	CNE	ANE	NE(d)
A	E	CE	AE	E(d)
	SE	CSE	ASE	SE(d)
	S	CS	AS	S(d)
	SW	CSW	ASW	SW(d)
	W	CW	AW	W(d)
	NW	CNW	ANW	NW(d)

allocation of WTs and in the number of unclassified days. Therefore, a sensitivity test is done using various numbers of grid points and different grid configurations. Originally, the grid was set up consisting of 16 grid points with a 10 resolution in zonal and a 5 resolution in meridional directions (Jenkinson and Collison, 1977). Eight sensitivity runs are set up here, differing in number of grid points (9, 16, 32) and grid resolution (2.5 , 5 and 10) (Figure 2). A sensitivity run with a 10 resolution on a 32-point grid is neglected because the area described by such a configuration exceeds our region of interest.

Overall, we can conclude that the number of unclassified days and the associated standard deviation decreases with a decreasing grid resolution (Table II). For the configuration with 16 and 32 grid points, a grid spacing of 2.5 is inappropriate leading to a large number of unclassified days, 155 and 136 days per year respectively (Table II). Also, for the configuration with nine gridpoints, a grid spacing of 2.5 is not appropriate: this grid configuration does not capture any circulation pattern (Table II), and classifies each day as pure anticyclonic, which explains the non-existence of unclassified days. From this it is clear that the grid-spatial scale needs to be related to the typical scale of synoptic circulation patterns. However, as differences between the 5 and 10 grid resolution using 16 grid points are small (25 and 19 respectively) and previous studies used the 16 grid points and 5 resolution, this study applies the same grid, enabling the opportunity to compare the results to former studies.

3.2. Evaluation of ECHAM5 SLP fields using ECMWF-ERA40 data

ECHAM5-MPI/OM SLP fields are evaluated using the reference CTL_{ERA40} dataset, for the December-January-February (DJF), March-April-May (MAM), June-July-August (JJA) and September-October-November (SON) seasons separately. Figure 3 shows the seasonal mean SLP of both models together with the absolute bias of the ECHAM5-MPI/OM normalized by the standard deviation of the ECMWF-ERA40 40-year time series for each season separately. The normalized bias is largest during summer and smaller during the winter season. This is due to the small inter-annual variability (as expressed by the standard deviation of the 40-year time series) during summer, which is related to the weak north–south pressure gradient during this season (van Ulden and van Oldenborgh, 2006). Therefore, the discrepancy in WTs between CTL_{ECHAM5} and CTL_{ERA40} is largest during summer, whereas during winter the WT occurrences correspond much better.

The patterns in ECHAM5-MPI/OM are overall similar compared to the ERA40 reference dataset, although differences can be noticed in the strength and location of the anticyclonic belts and low-pressure systems. The occurrences of the WTs in ECHAM5-MPI/OM correspond within 10% to the ECMWF-ERA40 occurrences for all seasons except the summer (Table III). During summer (JJA), there is an underestimation of the frequency of occurrence in CTL_{ECHAM5} of 4 and 5% for the NE(d) and E(d) directional groups, respectively, and an overestimation of 4 and 14% for the JJA SW(d) and W(d), respectively. This can be explained by an underestimation of ECHAM5-MPI/OM MSLP north of the British Isles, and a small overestimation of MSLP around the Mediterranean Sea (Figure 3(c)), associated with an increased North–South pressure gradient in ECHAM5-MPI/OM.

For DJF, CTL_{ECHAM5} shows an easterly geostrophic flow anomaly in the northern part and a westerly geostrophic flow anomaly in the southern part of the WT grid (Figure 3(a)). Note hereby that the WT grid is extending from the south of Norway to Sardinia (Figure 2). This results in anomalous cyclonic shear vorticity in our region of interest explaining the underestimation in anticyclonic WTs in CTL_{ECHAM5}. In addition, the North-South gradient in the WT grid increases, explaining the overestimation of western WTs in CTL_{ECHAM5} (Figure 3(a)).

For MAM, the location of an anomalous low-pressure system in CTL_{ECHAM5} west of the British Isles, results in a stronger pressure gradient in the north-west to south-east axis in our region of interest. This leads to an increase (decrease) of W(d) and SW(d) [E(d) and NE(d)] WTs (Figure 3(b)). As pressure differences are smaller for SON in the WT grid domain (Figure 3(d)),

Copyright © 2008 Royal Meteorological Society

DOI: 10.1002/joc

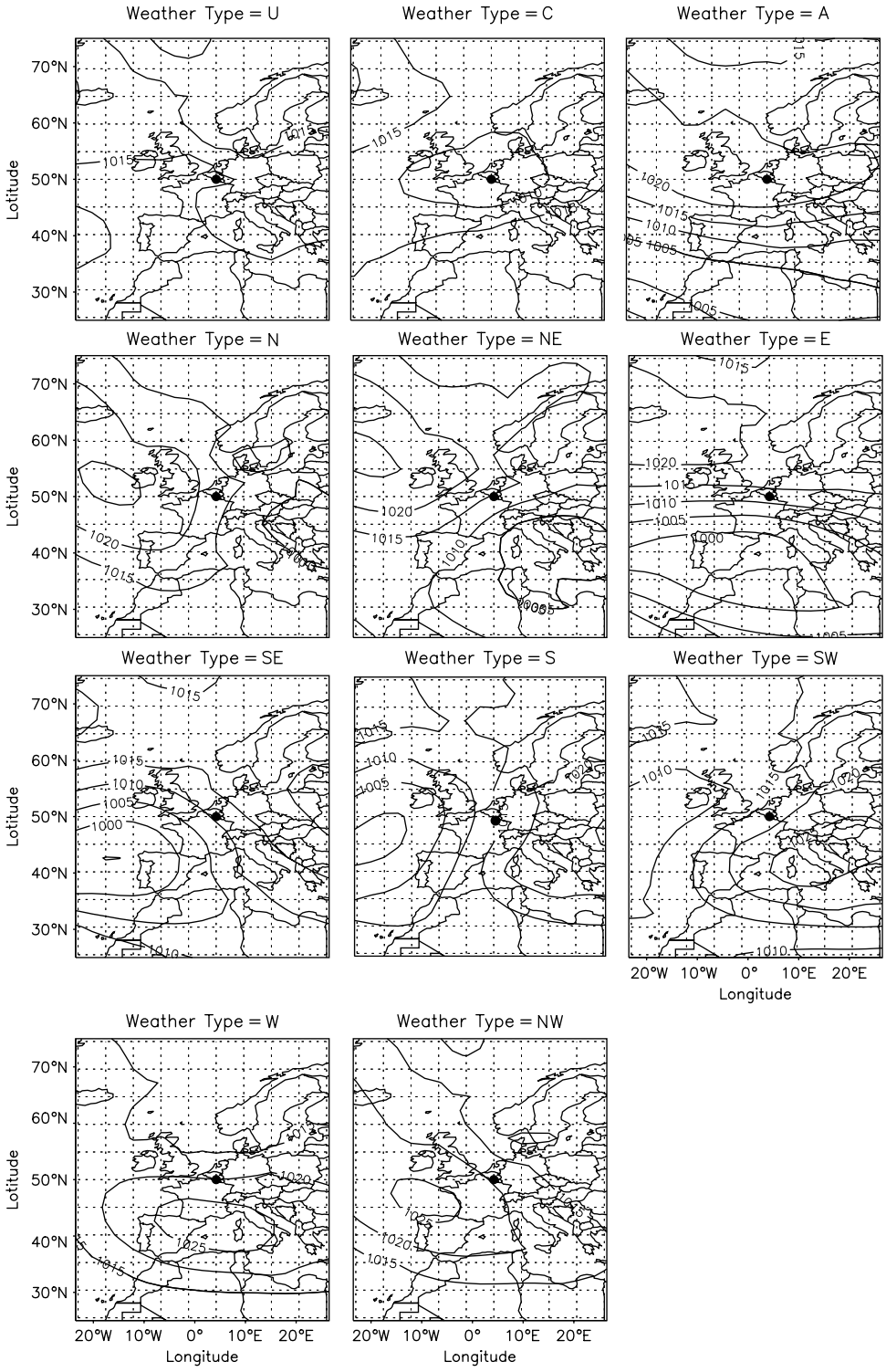

Figure 1. SLP composites for all directional Lamb weather types derived from the ECMWF-ERA40 SLP reference dataset, averaged over the period 1961–2000.

also WT frequency differences are lowest for this season (Table III).

In general, the more pronounced CTL_{ECHAM5} pressure gradients result in a lower number of unclassified days, both yearly and seasonal, which suggest that CTL_{ECHAM5} pressure patterns have more pronounced (unrealistic) circulation characteristics (Table III). Most significant differences (based on t-test statistics) between CTL_{ECHAM5} and CTL_{ERA40} are found in the late spring, summer and beginning of autumn (from May to September) (Table IV; Figure 4). During these seasons, WT occurrences of western types are significantly higher for CTL_{ECHAM5} than for CTL_{ERA40} and the occurrences of eastern types are lower. This corresponds to the results of van Ulden and van Oldenborgh (2006), who tested various global coupled climate models with respect to the explained variance in

Copyright © 2008 Royal Meteorological Society

DOI: 10.1002/joc

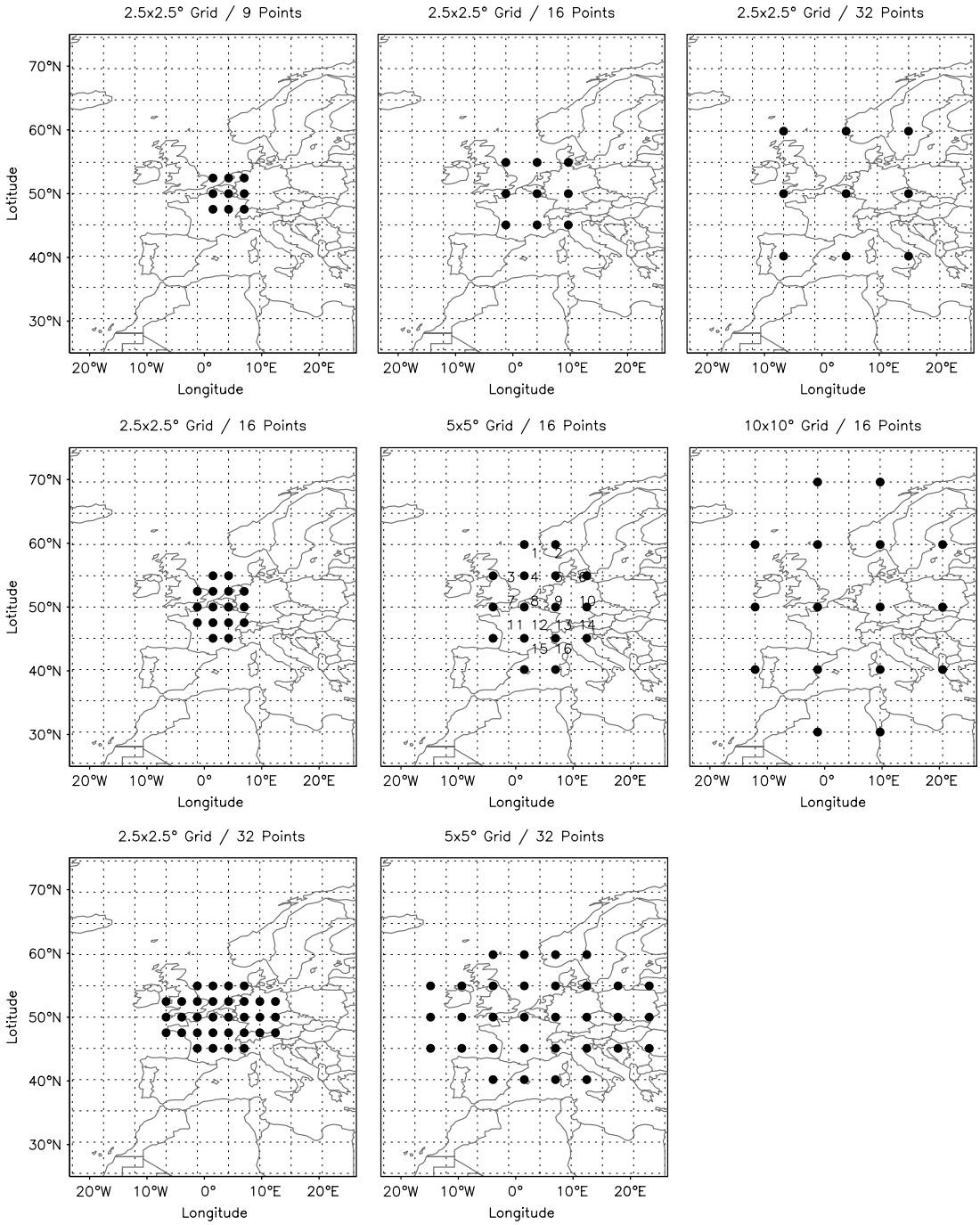

Figure 2. Visualization of the grid for the different sensitivity runs. Upper row: 9 grid points 2.5 , 5 , 10 ; middle row: 16 grid points on 2.5 , 5 , 10 ; lower row: 32 grid points on 2.5 and 10 . Grid points are labelled only for the central plots from 1 to 9, 1 to 16 and 1 to 32 for the 9, 16 and 32 number of points plots respectively.

SLP for northern latitudes (their Figure 2). They found that ECHAM5-MPI/OM, next to others, has difficulties in correctly simulating circulations from April to September. These discrepancies could be due to the fact that the ECHAM5-MPI/OM does not use flux adjustment (as compared to other models), and therefore, model bias in SST can be expected which will also affect circulation patterns. van Ulden and van Oldenborgh (2006) tested various IPCC AR4 models in terms of circulation. ECHAM5-MPI/OM was shown to be one of the best models, although also here summer circulations in northern latitudes (30–90 N) are shown to be difficult to simulate correctly. Moreover, a comparison to a flux adjusted model (MIROchi – their Figure 18) showed that the latter was better in simulating the explained spatial variance in SLP, compared to the other non-flux adjusted models, including ECHAM5. Also the model resolution should be taken into account. Roeckner *et al.* (2006a) found that the JJA westerly wind bias around 50 N is still present at T106L31 resolution but clearly smaller than at the resolution used in our study (see their Figure 10).

Copyright © 2008 Royal Meteorological Society

DOI: 10.1002/joc

Table II. Averaged number and standard deviation per year of unclassified days for the 1961–2000 period, for a grid configuration with 9, 16 or 32 grid points and a resolution of 2.5, 5 or 10 .

Grid points		9			16			32
Resolution	**2.5**	**5**	**10**	**2.5**	**5**	**10**	**2.5**	**5**
Mean	–	62	21	155	25	19	136	35
Standard deviation	–	9	6.25	14.64	5.94	4.19	14.25	6.59

The difference in frequency distribution of WTs between CTL_{ECHAM5} and CTL_{ERA40} is assessed using the χ^2 test. During the summer season, CTL_{ECHAM5} distribution of WTs significantly differs from CTL_{ERA40} (Table V). During spring, autumn and winter both populations are not significantly different. On a monthly scale, significant differences between CTL_{ECHAM5} and CTL_{ERA40} are revealed in May and July WT frequencies (Table V).

Additionally, WTs are derived removing the systematic errors in ECHAM5-MPI/OM prior to doing the classification. Firstly, the monthly mean 40-year bias is calculated as the difference between ECHAM5-MPI/OM and ECMWF-ERA40 SLP. Secondly, the WTs are derived after subtracting this bias from the original daily ECHAM5-MPI/OM SLP. There is a significant impact of eliminating the biases on the WT classification (Table VI). The variability in WTs in Western Europe is very well presented by ECHAM5 once the systematic errors in SLP are removed: There is no significant difference in terms of mean annual, seasonal and monthly WT frequencies between ECMWF-ERA40 and the bias-corrected ECHAM-MPI/OM SLP (Table VI). Therefore, it is concluded that the discrepancy in WT occurrences between ECHAM5-MPI/OM and ECMWF-ERA40 can be explained by the monthly mean bias.

For each month, the mean bias for all WTs over the 40-year period is calculated. This bias presents the mean difference in number of occurrences (days) between CTL_{ECHAM5} and CTL_{ERA40} calculated for each month separately over all directional WTs (Table IV, right column). Biases are largest for May and July (1.24 and 1.26 days respectively). For all months from May to September, biases are exceeding a value higher than 1 day (Table IV). For the remaining months, values are lower than 1 (day). On the basis of the significant differences on a monthly and seasonal time scale from Table IV, and taking into account this value of 1 day as a threshold, we conclude that ECHAM5-MPI/OM generally reproduces the observed WTs quantities for the October-November-December-January-February-March-April (ONDJFMA) months for the period 1961–2000. Non-negligible differences for the May-June-July-August-September (MJJAS) period are found, where CTL_{ECHAM5} overestimates (underestimates) the number of westerlies (easterlies). Therefore, in order to avoid the model uncertainties concerning MJJAS circulation patterns in the ensuing analysis, our further analyses are restricted to the ONDJFMA period.

In Figure 5, MSLP composites are plotted for the years 1961–2000, for the ONDJFMA period. Generally, the SLP shows similar patterns for CTL_{ECHAM5} and CTL_{ERA40}, although values differ regionally. The CTL_{ECHAM5} run overestimates pressure over the Sahara region and northern parts of Scandinavia, with pressure differences up to 2.5 and 3.0 hPa, respectively, whereas pressure patterns are slightly underestimated from Central Europe to the North-west region of Ireland, with differences up to 3 hPa. Generally, the pressure differences between CTL_{ECHAM5} and CTL_{ERA40} are small over the WT grid, and therefore differences in WTs are small for these months. Note that there are no significant trends in WT occurrence over the 40-year period in ERA40.

3.3. The relation between weather types and other indices of large-scale flow

Since the NAO-index, cyclone identification and blocking indices are often used to characterize atmospheric flow conditions in Western and Central Europe; in this section we compare these measures with the WT method to evaluate climate models. Many authors have proposed methods to calculate NAO indices, based on (normalized) the pressure differences between stations pairs, area-weighted pressure extremes or principal component time series corresponding to a pressure field principal component pattern (Osborn *et al*., 1999 – references therein). Some authors (Ulbrich and Christoph, 1999; Hu and Wu, 2004) show that the largest values in teleconnectivity do not coincide with the reference locations used in the NAO index definition provided by Hurrell (1995). In addition, they point out a shift in the NAO action centres in global warming climate simulations. Latif *et al*. (2000) confirm this with a canonical correlation analysis applied on ECHAM4. Their analysis reveals a north-eastward shift in the NAO centres of action. As pointed out by Campbell *et al*. (1995) and Huth (1997), there is a lack of consensus on the spatial NAO characteristics. This is especially relevant for studying changes in the NAO, as the shift in the NAO action centres depends on the methods used to characterize the NAO. It is, however, of lesser importance here, as the aim of our analysis is to relate the present-day NAO with present-day SLP circulation patterns. For such an analysis, the precise definition of an index is of less importance provided that the comparison is performed on an identical basis (Osborn *et al*., 1999). Indices derived for longer time scales show that the NAO is the best discerned when time-averaged (monthly or, preferably, seasonal) atmospheric fields are analysed (Marshall, 2001; Loptien and Ruprecht, 2005). Therefore, the seasonal DJF NAO index is derived from both

Copyright © 2008 Royal Meteorological Society

DOI: 10.1002/joc

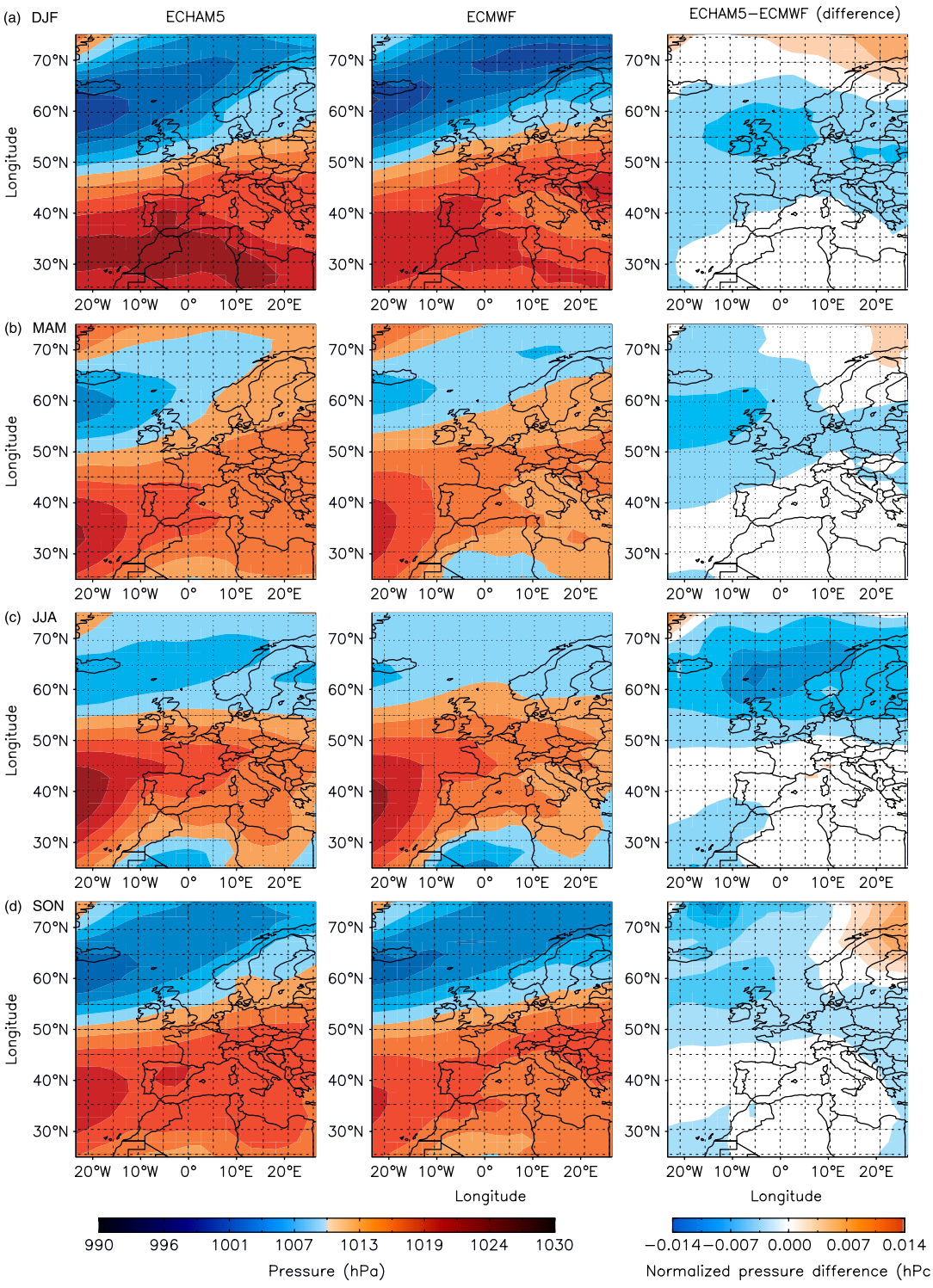

Figure 3. Mean sea level pressure during the period 1961–2000, based on ECHAM5-MPI/OM (left column), ECMWF-ERA40 (middle column) and the difference between the two (right column), normalized by the standard deviation. This is done for each season separately (consecutive (a) DJF, (b) MAM, (c) JJA and (d) SON). This figure is available in colour online at www.interscience.wiley.com/ijoc

ECMWF-ERA40 and ECHAM5-MPI/OM by calculating the difference of normalized SLP from the nearest grid boxes to the Ponta Delgada (Azores) and the Stykkisholmur (Iceland) measurement sites (Figure 6). In addition, the NAO index based on the measurements from Hurrell (1995) is added as the reference NAO index (Figure 6).

Pearson correlation coefficients are calculated between the DJF frequencies of WTs and the DJF NAO index, both for CTL_{ERA40} and ECHAM5-MPI/OM (Table VII). There is a strong significant negative correlation between the DJF NAO index and both CTL_{ERA40} and CTL_{ECHAM5} cyclonic WTs. This can be explained by a northward shift of cyclone activity (above 60 N) during winters with a positive winter NAO index (Sickmöller *et al.*, 2000; Raible and Blender, 2004; Raible *et al.*, 2005). Since the northern boundary of the WT grid is located at 60 N, our

Copyright © 2008 Royal Meteorological Society

DOI: 10.1002/joc

Table III. Mean annual and seasonal frequency differences (in days and %) of all groups of directional circulation types for ECHAM5 minus ERA40 between 1961 and 2000.

	Annual		Winte (DJF)		Spring (MAM)		Summer (JJA)		Autumn (SON)	
	Days	(%)	Days	(%)	Days	(%)	Days	(%)	Days	(%)
U	−10.2	*−2.8*	0.4	*0.4*	−2.4	*−2.6*	−6.1	*−6.6*	−2.2	*−2.4*
C	2.3	*0.6*	3.7	*4*	0.2	*0.2*	−1.7	*−1.9*	0.2	*0.2*
A	−16.3	*−4.5*	−7.6	*−8.4*	−1.5	*−1.7*	−0.8	*−0.9*	−6.3	*−7*
N(d)	−7.3	*−0.9*	−0.2	*−0.3*	−0.9	*−0.9*	−1.3	*−1.3*	−0.9	*−0.9*
NE(d)	−9.8	*−2.7*	−1	*−1.2*	−4	*−4.3*	−3.5	*−3.8*	−1.4	*−1.5*
E(d)	−9.7	*−2.6*	−2.9	*−3*	−2.6	*−2.7*	−4.3	*−4.7*	0	*0.2*
SE(d)	0.7	*0.2*	−0.9	*−0.9*	0.8	*0.8*	−0.2	*−0.2*	0.9	*1*
S(d)	1.3	*0.3*	0	*0.1*	0.7	*0.7*	0.6	*0.7*	0	*0*
SW(d)	10.8	*3*	0.9	*1*	5	*5.4*	3.7	*4*	1.3	*1.5*
W(d)	32.5	*8.9*	7.4	*8.2*	5.2	*5.7*	12.8	*14*	7	*7.8*
NW(d)	1.2	*0.5*	0.1	*0.1*	−0.6	*−0.6*	0.8	*0.8*	1	*1.3*

Table IV. Monthly frequency differences (in days averaged over 40 years) for all groups of WTs for ECHAM5 minus ERA40.

	U	C	A	N(d)	NE(d)	E(d)	SE(d)	S(d)	SW(d)	W(d)	NW(d)	Bias(days/month)
Jan	−0.07	**2.07**	−2.05	0.09	−0.05	−0.49	−0.19	0.19	−0.42	1.21	−0.3	0.65
Feb	−0.28	1.14	−1.88	−0.23	−0.7	−1.23	−0.21	−0.28	1	2.79	−0.12	0.9
Mar	0.37	−0.09	−1.81	0.05	−0.33	0.26	0.49	0.26	1.84	−0.07	−0.95	0.59
Apr	−0.84	0.33	0.26	−0.49	**−2.07**	−0.35	0.4	0	1.23	1.56	−0.02	0.68
May	**−1.65**	0	−0.02	−0.37	**−1.72**	**−2.81**	−0.23	0.35	**2.02**	**3.84**	0.6	1.24*
Jun	−1.02	−0.49	−0.19	−0.37	**−1.88**	**−1.72**	0.09	0.21	1.09	**3.42**	0.86	1.03*
Jul	**−2.05**	**−0.44**	−1.23	**−0.42**	**−1.05**	**−1.65**	−0.12	**0.4**	**1.51**	**5**	0.05	1.26*
Aug	**−2.88**	−0.98	0.56	−0.26	−0.47	−0.72	−0.21	0.12	**1.05**	**3.88**	−0.09	1.02*
Sep	**−2.09**	−0.3	**−1.84**	−0.05	−0.49	−0.77	**0.14**	0.07	1.26	**3.56**	0.51	1.01*
Oct	−0.42	−0.12	−1.42	−0.44	−0.09	0.47	0.4	0.16	0.09	0.95	0.42	0.45
Nov	−0.28	0.47	−2.67	−0.28	−0.6	0.14	0.23	−0.21	−0.3	**3.33**	0.19	0.79
Dec	0.47	0.42	**−3.44**	−0.05	−0.35	−0.95	−0.21	0.09	0.47	3.16	0.4	0.91

Significant differences on the 99% level are denoted in bold. The bias presents the differences in monthly frequencies (days per month) averaged over all years for all types (CTL_{ECHAM5} minus CTL_{ERA40}). Months with a yearly averaged bias >1 are denoted by *.

WT classification method is not capturing the increase in cyclonic activity north of 60 N during a positive NAO phase. Our results confirm the findings of Sickmöller *et al.* (2000) who state that clustered cyclone based on their occupation [north-eastward (NE), zonal (ZO) and stationary (ST)] shows clear negative correlations with NAO for their NE and ZO cyclone clusters over Central Europe.

Scherrer *et al.* (2006) have shown, next to others, that there is a positive correlation between three blocking indices and a positive NAO phase. This is consistent with the significant positive correlation between NAO and anticyclonic WTs for both CTL_{ERA40} and CTL_{ECHAM5} (Table VII). The underestimation of the correlation coefficient in CTL_{ECHAM5} is due to an underestimation of anticyclonic WTs frequencies in CTL_{ECHAM5} compared to CTL_{ERA40} (Table III). The slope of the regression curve between anticyclonic WT frequency and NAO index is similar in CTL_{ECHAM5} compared to CTL_{ERA40} (Figure 7(a)).

The directional western WT correlates positively with the winter NAO index (Table VII), but the correlation is only significant at the 90% level for CTL_{ERA40} and not

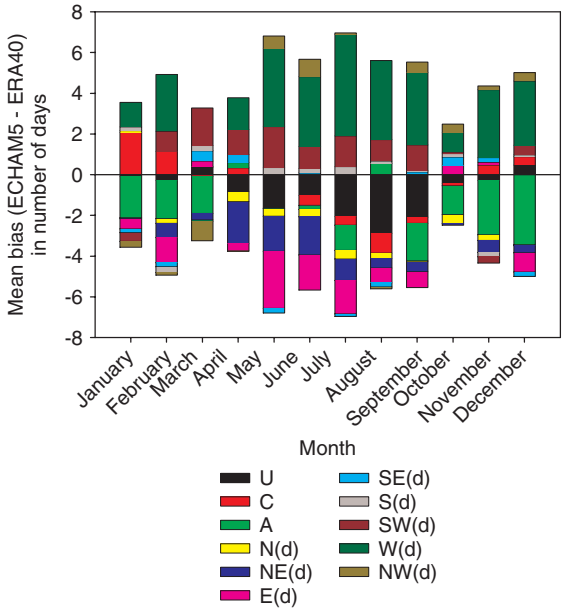

Figure 4. Mean monthly bias for each individual directional weather type, for each month between 1961 and 2000, calculated as the difference between ECHAM5 and ECMWF-ERA40. This figure is available in colour online at www.interscience.wiley.com/ijoc

Copyright © 2008 Royal Meteorological Society

DOI: 10.1002/joc

Table V. Statistical analysis between observed and expected frequencies of WTs during the 1961–2000 period.

	Year	Season	Month
Dec			0.33
Jan		0.20	0.98
Feb			0.60
Mar			0.82
Apr		0.25	0.62
May	**0.55×10^{-3}**		**4.6×10^{-2}**
Jun			0.11
Jul		**4×10^{-3}**	**5.5×10^{-2}**
Aug			0.28
Sep			0.19
Oct		0.42	0.77
Nov			0.49

Values <0.1 allow the hypothesis that CTL_{ECHAM5} is a good approximation of CTL_{ERA40} to be rejected (both populations are significantly different) and are marked in bold.

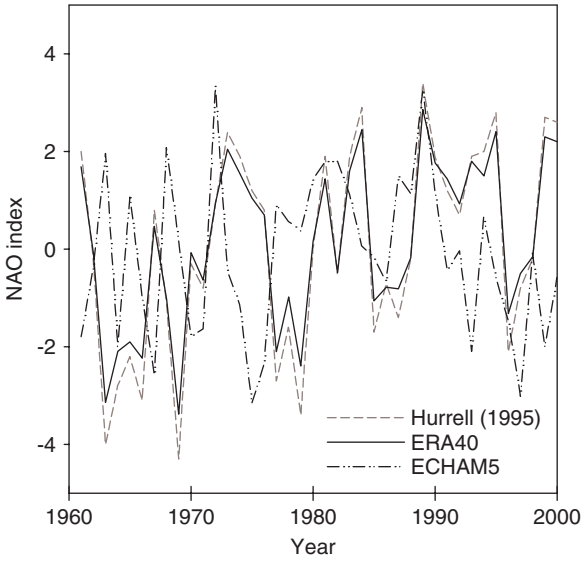

Figure 6. The station-based NAO index from Hurrell (1995) and derived from ERA40 and ECHAM5-MPI/OM as the difference of normalized sea level pressure from the nearest grid boxes to the Ponta Delgada (Azores) and Stykkisholmur (Iceland) between DJF 1961 and 2000. This figure is available in colour online at www.interscience.wiley.com/ijoc

for CTL_{ECHAM5}. Figure 7(b) shows that not only the correlation coefficient, but also the slope of the regression between western directional type W(d) and NAO index differs, even though the mean pressure patterns anomalies during the positive NAO years (NAO+) and negative NAO years (NAO−) (Figure 8) are almost identical. To analyse this in more detail, the regression between the mean yearly indices SF, WF, FF and Z of the WT method (see Section on 2.2) and the NAO index for CTL_{ECHAM5} and CTL_{ERA40} are calculated (not shown). There is no difference in the slope of the regression between geostrophic flow indices SF, WF and FF and NAO index between ECHAM5-MPI/OM and ECMWF-ERA40. Contrarily the vorticity index Z shows a less negative slope in CTL_{ECHAM5} compared to CLT_{ERA40}. Note that such a difference between CTL_{ECHAM5} and CLT_{ERA40} in the sensitivity of the shear vorticity to the NAO index can also be identified from Figure 8. Since the sensitivity of Z to the NAO index is underestimated in CTL_{ECHAM5}, the sensitivity of C to the NAO index is slightly underestimated as well. This is compensated by a slight underestimation of the sensitivity to NAO index of W(d), SE(d) and E(d) (Table VII; Figure 7(b)).

On the one hand, our approach confirms the results of many authors who have already shown that a positive NAO corresponds to an enhanced zonal flow over Central Europe with an anomalously low (high) pressure over the subpolar (subtropical) North Atlantic (Hoerling *et al.*,

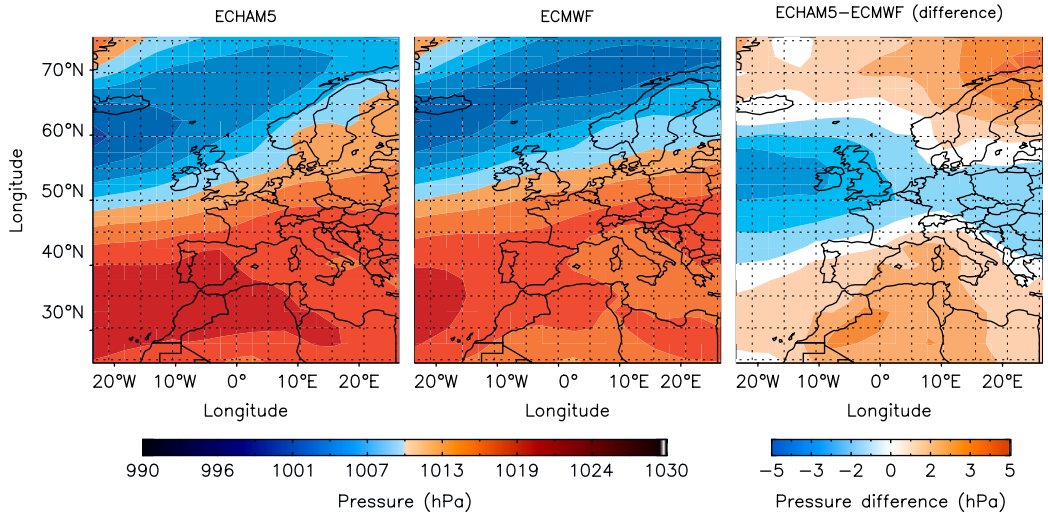

Figure 5. Mean sea level pressure averaged over the period 1961–2000, for the ONDJFMA period only. The ECHAM5-MPI/OM SLP pattern is shown in the left panel, ECMWF-ERA40 in the middle and the difference between the two in the right panel. This figure is available in colour online at www.interscience.wiley.com/ijoc

Copyright © 2008 Royal Meteorological Society

DOI: 10.1002/joc

Table VI. Same as Table III, but using ECHAM5 SLP with a monthly bias-correction.

	Annual		Winter (DJF)		Spring (MAM)		Summer (JJA)		Autumn (SON)	
	Days	(%)	Days	(%)	Days	(%)	Days	(%)	Days	(%)
U	−4.59	*−1.3*	−0.28	*−0.1*	−0.43	*−0.1*	−1.64	*−0.4*	−2.24	*−0.6*
C	−0.98	*−0.3*	1.29	*0.4*	−0.74	*−0.2*	−1.23	*−0.3*	−0.30	*−0.1*
A	0.93	*0.3*	−0.24	*−0.1*	1.42	*0.4*	1.30	*0.4*	−1.56	*−0.4*
N(d)	0.73	*0.2*	0.12	*0.0*	0.53	*0.1*	0.63	*0.2*	−0.56	*−0.2*
NE(d)	−2.63	*−0.7*	−0.18	*0.0*	−1.72	*−0.5*	−0.09	*0.0*	−0.64	*−0.2*
E(d)	1.11	*0.3*	−0.82	*−0.2*	−0.34	*−0.1*	0.64	*0.2*	1.64	*0.4*
SE(d)	0.67	*0.2*	−0.64	*−0.2*	−0.20	*−0.1*	0.39	*0.1*	1.12	*0.3*
S(d)	−0.19	*−0.1*	0.22	*0.1*	−0.26	*−0.1*	0.34	*0.1*	−0.48	*−0.1*
SW(d)	−1.94	*−0.5*	−1.12	*−0.3*	0.24	*0.1*	−0.13	*0.0*	−0.93	*−0.3*
W(d)	3.81	*1.0*	1.71	*0.5*	1.02	*0.3*	−1.52	*−0.4*	2.60	*0.7*
NW(d)	3.0	*0.8*	−0.1	*0.0*	0.5	*0.1*	1.3	*0.4*	1.4	*0.4*

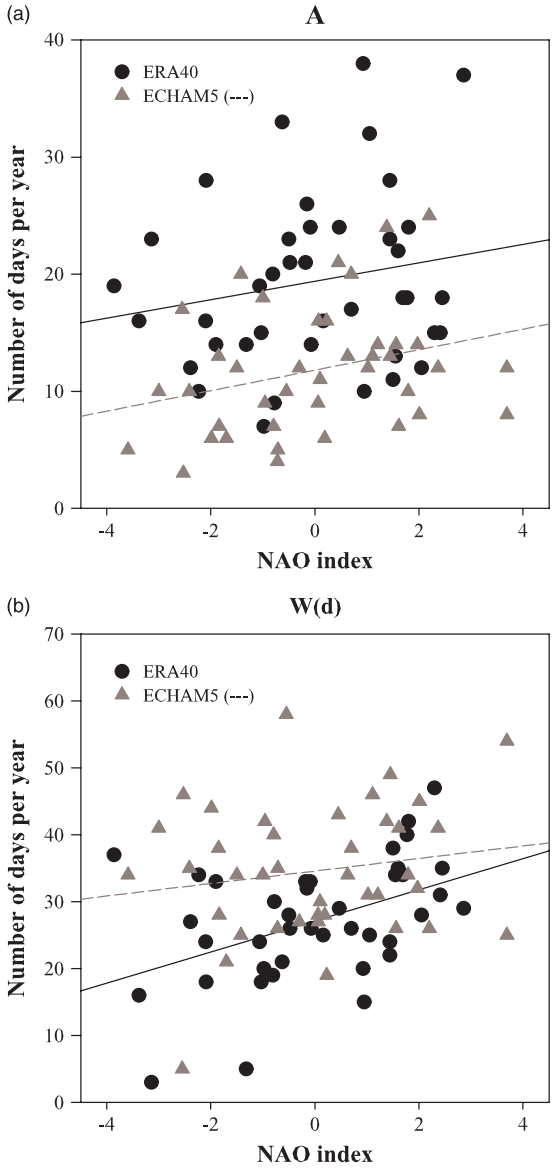

Figure 7. Mean frequencies of the (a) A and (b) W(d) weather types (in mean number of days per year) against the NAO index, plotted with an ascending NAO index. This figure is available in colour online at www.interscience.wiley.com/ijoc

2001) (Figure 8). On the other hand, it clearly points out the additional value of using this WT approach as a diagnostic evaluation tool for CGCMs. Not only it captures large-scale features found by other authors combining a multiple set of methods (NAO index, cyclone algorithms, blocking indices), but also shows that although pressure pattern differences between NAO+ and NAO− are similar for CTL_{ERA40} and CTL_{ECHAM5} (Figure 8), one should also check the frequency of occurrence of the large-scale circulation patterns, which can be easily done using the WT method.

3.4. Climatic trends in weather types

In this section, ECHAM5-MPI/OM climate change experiments with observed atmospheric greenhouse and aerosol concentrations since 1860 and different assumptions on future greenhouse gas and aerosol concentrations are discussed, namely the IPCC scenarios A1B, B1, and A2 until the year 2100. Following the IPCC report 2001, scenario A1B describes the future with a fast economic growth, a world population that peaks in the mid-century and declines afterwards and new and more efficient technologies. The scenario B1 is described by a similar population curve as A1B, but with an emphasis on global solutions to economic, social and environmental sustainability, including improved equity. The last scenario A2 differs herein that population continues growing through the century with a regionally developing economic growth and fragmented technological changes (IPCC, 2001).

For each WT group and scenario, the yearly mean number of occurrences is calculated for the 2001–2100 ONDJFMA period ($SCEN_{A1B-Coupled}$, $SCEN_{B1-Coupled}$ and $SCEN_{A2-Coupled}$). Trends are calculated for the eight directional and two pure (anti) cyclonic WT groups between 2001 and 2100 and for the various scenarios A1B, B1 and A2. Regression analyses for directional groups N(d), NE(d), SE(d), S(d), SW(d) and NW(d) show no significant trend over the whole time period (not shown). The (anti) cyclonic and W(d) and E(d) series of occurrences and their linear trends are shown

Copyright © 2008 Royal Meteorological Society

DOI: 10.1002/joc

Table VII. Correlation between the NAO index and the CLT_{ERA40} and CTL_{ECHAM5} directional WTs frequencies using ERA40 NAO and ECHAM5-MPI/OM NAO, this for DJF.

	U	C	A	N(d)	NE(d)	E(d)	SE(d)	S(d)	SW(d)	W(d)	NW(d)
DJF											
ERA40	−0.031	**−0.37**	0.19	−0.04	−0.24	**−0.28**	**−0.37**	−0.17	0.006	**0.45**	−0.01
ECHAM5	0.11	**−0.27**	**0.29**	0.02	−0.07	−0.15	0.11	−0.21	−0.21	0.17	−0.05

Values on a 90% significance level are denoted in bold.

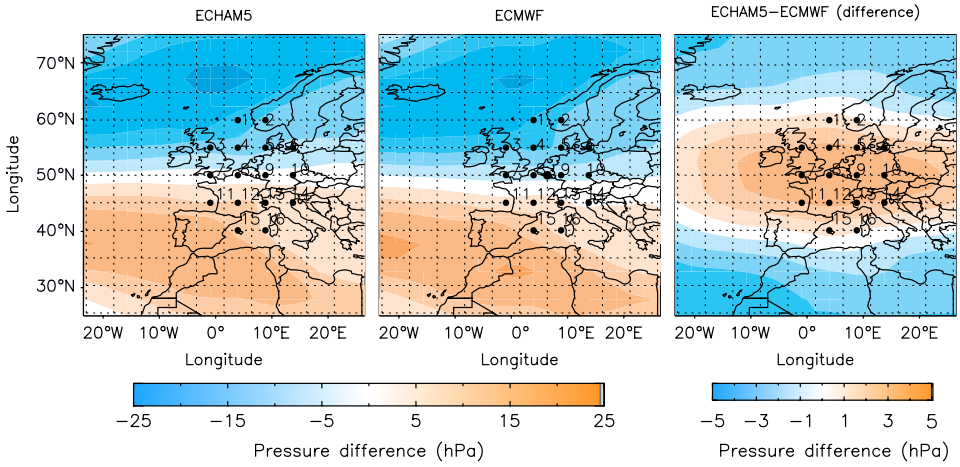

Figure 8. Mean SLP differences between NAO+ and NAO− years (for DJF), for CTL_{ECHAM5} (left panel) and CLT_{ERA40} (middle panel) and $CTL_{ECHAM5} - CLT_{ERA40}$ (right panel). This figure is available in colour online at www.interscience.wiley.com/ijoc

in Figure 9. Within each directional WT group, trends for scenarios A1B, B1 and A2 are similar over the whole period, as well in amplitude as in overall trend. Year-to-year variability is large, as one could expect. Because long-term differences between the various scenario trends based on WTs are small, this study will continue its focus only on the scenario A1B. Trends have been re-calculated for the A1B scenario over the whole 240-year period, expanding from 1860 to 2100, selecting only ONDJFMA months (Figure 10).

Thereby, we can see an increase in number of the western directional type, balanced by a smaller decrease of pure cyclonic and all eastern directional WTs. The Mann-Kendall test is applied to test the trends' significance. For the representative directional and the two pure cyclonic WTs, the Mann-Kendall trend test P-values and linear trends are given (Table VIII).

The statistical analyses show that the increasing (decreasing) trend in all-West (all-East) is determined to a large extent by a significant increase in pure West directional types (by a decrease in pure East directional types) (Table VIII). The increase of W(d) results in an absolute mean increase of almost 73 extra days over 240 years of westerly flow W(d) over Central Europe during the months ONDJFMA. Again, a large year-to-year variability is found for all directional groups.

4. Conclusions

Until now, only few studies have tackled the strength of CGCMs in reproducing circulation patterns. In this respect, the automated WT classification method is tested as a diagnostic tool to evaluate CGCMs for the Western and Central European Region. The WTs for a 40-year control run (1961–2000) of the ECHAM5-MPI/OM CGCM for Western and Central Europe are evaluated using the ECMWF-ERA40 database. In general, ECHAM5-MPI/OM appears to be able to reproduce the frequencies in directional circulation types, especially for the late autumn, winter and early spring period ONDJFMA. For late spring, summer and early autumn (MJJAS), significant differences are found for most of the directional types. In particular western types are significantly overestimated by ECHAM5-MPI/OM, while eastern types are underestimated.

As the NAO climate variability is of large interest for the Western and Central European climate, this large-scale teleconnection pattern is compared to the WTs for the DJF winter period. The NAO index is positively correlated with the frequency of occurrence of westerly WTs whereby our approach confirms the results obtained by earlier research that a positive NAO phase is characterized by a stronger zonal flow, due to positive (negative) pressure anomalies over the subtropical (subpolar) ocean (Hoerling *et al*., 2001). Furthermore, a positive relation between the NAO+ phase and blocking over Central Europe, as shown by Scherrer *et al*. (2006), is recognized by our classification approach: the relation between the frequency of occurrence of the anticyclonic WT and the NAO index is positive. The negative correlations between cyclones and the NAO index as found by Sickmöller *et al*. (2000) are confirmed by a negative correlation

Copyright © 2008 Royal Meteorological Society

DOI: 10.1002/joc

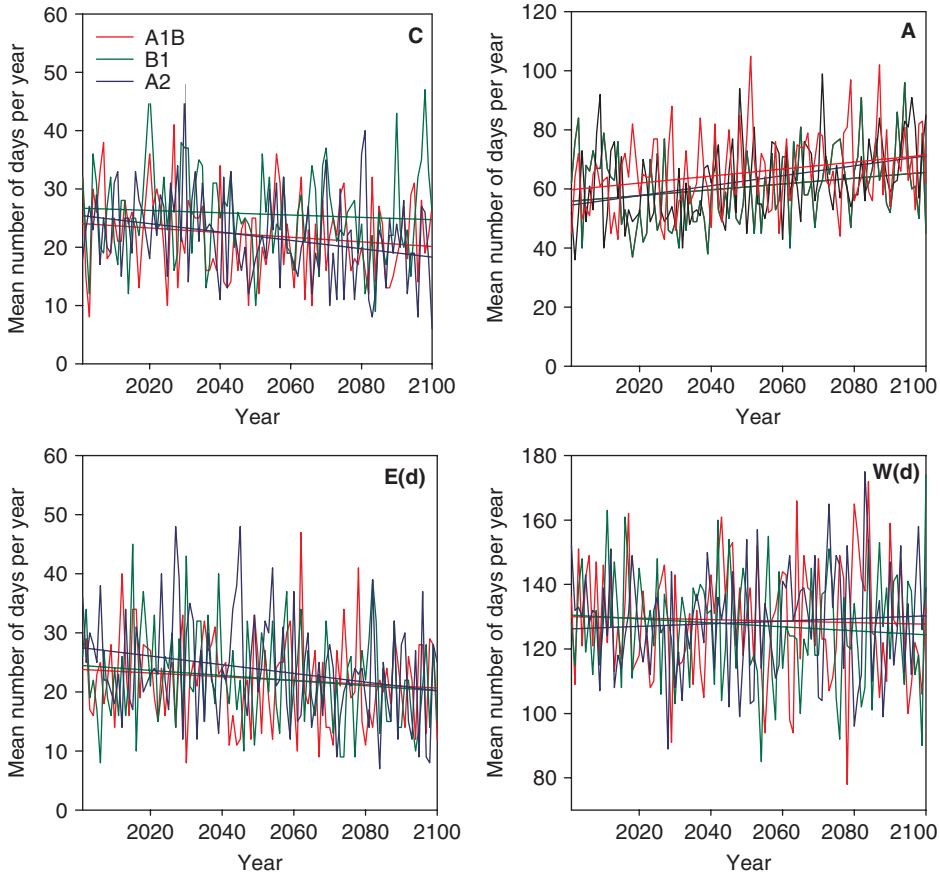

Figure 9. Mean number of days per year with weather types C, A, W(d) and E(d) for the $SCEN_{A1B-Coupled}$ (red), $SCEN_{B1-Coupled}$ (green) and $SCEN_{A2-Coupled}$ (blue) simulations with ECHAM5-MPI/OM from 2000 to 2100, for the ONDJFMA period only. The bold line in its respective colour denotes the trends for the different scenarios. This figure is available in colour online at www.interscience.wiley.com/ijoc

Table VIII. The Mann-Kendall rank test is used to calculate significance of the $SCEN_{A1B\ -\ Coupled}$ circulation trends between the 1860–2100 period (ONDJFMA)..

Type	C	A	N(d)	NE(d)	E(d)	SE(d)
Linear trend	−5.807	2.489	−0.11	−1.11	−4.3	−1.6
Mkprob	**0.000106***	0.252208	0.284108	**0.025138**	**0.002343***	0.127748
Type	S(d)	SW(d)	W(d)	NW(d)	All West	All East
Linear trend	0.201	1.512	11.91	−1.2	12.22	−7.011
Mkprob	0.878028	0.3939	**0.00034***	**0.066631**	**0.001055***	**0.001689***

90% level of significance is indicated in bold, 95% level by * .

between the frequency of occurrence of the cyclonic WT C and the NAO index.

In order to avoid model deficiencies in the analyses of potential future changes of circulation patterns, ECHAM5-MPI/OM climate scenarios are tested for the ONDJFMA period, only. Although inter-annual variability between the A1B, B1 and A2 IPCC scenario schemes is large, the trends for the circulation types between 2000 and 2100 using the three IPCC scenarios are similar. The Mann-Kendall test is used to calculate the $SCEN_{A1B-Coupled}$ circulation trends between 1860 and 2100. While in general the trends for the directional groups are insignificant, there is a significant increase (decrease) in western (eastern) directional groups. This suggests that one can expect a larger influence of western circulation over Central Europe during future autumn and winter seasons. However, one should keep in mind that the used ECHAM5-MPI/OM model showed the largest deviations from the ECMWF-ERA40 data for exactly the same circulation patterns, W(d) and E(d), during the summer months. Thus, further analyses and general circulation model (GCM) inter-comparison studies are certainly needed to test the robustness of the detected future circulation changes.

Copyright © 2008 Royal Meteorological Society

DOI: 10.1002/joc

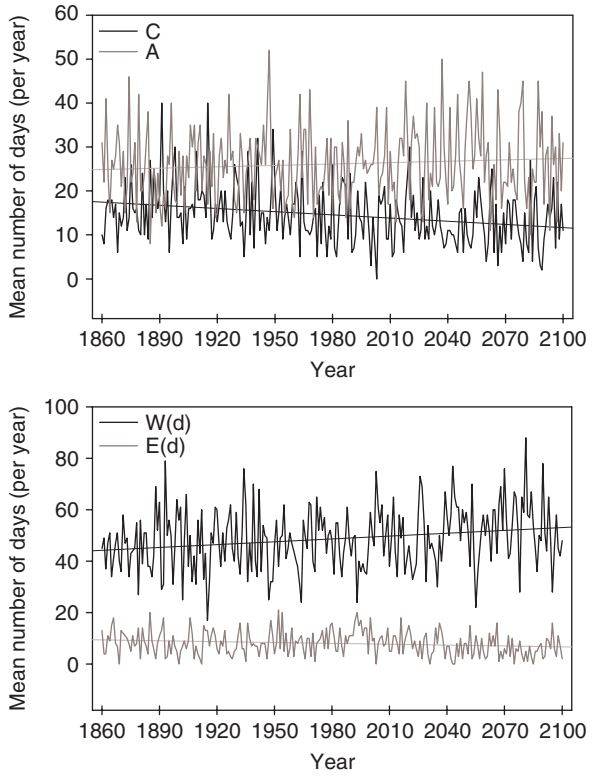

Figure 10. Same as Figure 9, but for the $SCEN_{A1B-Coupled}$ run and the 1860–2100 ONDJFMA period only. This figure is available in colour online at www.interscience.wiley.com/ijoc

In order to increase the reliability of CGCMs in future projections, down-scaling, air quality monitoring, boundary conditions for regional climate models and other applications, one has to make sure that overall circulation patterns are projected with confidence in all seasons. Thus, the approach suggested here could provide a rather simple methodology to detect changes and differences in circulation patterns on a synoptic time scale, which makes WT-scheme as an appropriate tool for CGCM evaluation. A lot of research has already been done on the NAO-related climatic impacts (see Marshall *et al*., 2001 and references therein), as well as on cyclone activity and blocking. On the basis of an automated classification method, as presented in this paper, climate impacts for various regions and on a synoptic time scale could easily be investigated for present-day climate and future CGCM scenarios. Thereby, further work is underway to extend the present analysis on its implications on regional surface climate variables (Trigo *et al*., 2002, 2004) as precipitation (Hurrell *et al*., 2004) and temperature (Schär *et al*., 2004).

Acknowledgements

This research is funded by a PhD grant of the Institute for the Promotion of Innovation through Science and Technology Flanders and the COST Office (action 733 on Harmonization and Applications of weather types Classifications for European Regions). ERA40 reanalysis data were provided by ECMWF (available at http://data.ecmwf.int/data/index.html). Furthermore we would like to thank Dr Martin Werner for his constructive supervision during the COST-STSM stay of M. Demuzere at the Max-Planck-Institute for Biogeochemistry in Jena. Also, we would like to thank the anonymous reviewers, for their valuable comments and suggestions.

References

Buchanan CM, Beverland IJ, Heal MR. 2002. The influence of weather-type and long-range transport on air particle concentrations in Edinburgh, UK. *Atmospheric Environment* **36**: 5343–5354.

Buishand A, Brandsma T. 1997. Comparison of circulation classification schemes for predicting temperature and precipitation in The Netherlands. *International Journal of Climatology* **17**: 875–889.

Campbell GG, Kittel TGF, Meehl GA, Washington. WM. 1995. Low-frequency variability and Co2 transient climate-change.2. Eof analysis of Co2 and model-configuration sensitivity. *Global and Planetary Change* **10**: 201–216.

Chernoff H, Lehmann EL. 1954. The use of maximum likelihood estimates in χ^2 tests for goodness-of-fit. *Annals of Mathematical Statistics* **25**: 579–586.

Conway D, Jones PD. 1998. The use of weather types and air flow indices for GCM downscaling. *Journal of Hydrology* **213**(1–4): 348–361.

D'Andrea F, Tibaldi S, Blackburn M, Boer G, Déqué M, Dix MR, Dugas B, Ferranti L, Iwasaki T, Kitoh A, Pope V, Randall D, Roeckner E, Straus D, Stern W, Van den Dool H, Williamson D. 1998. Northern Hemisphere atmospheric blocking as simulated by 15 atmospheric general circulation models in the period 1979–1988. *Climate Dynamics* **14**(6): 385–407.

Fowler HJ, Kilsby CG. 2002. A weather-type approach to analyzing water resource drought in the Yorkshire region from 1881 to 1998. *Journal of Hydrology* **262**: 177–192.

Goodess CM. 2000. The construction of daily rainfall scenarios for Mediterranean sites using a circulation-type approach to downscaling. *PhD Thesis, University of East Anglia*, Norwich, UK, 486.

Hoerling MP, Hurrell JW, Xu TY. 2001. Tropical origins for recent North Atlantic climate change. *Science* **292**: 90–92.

Hu ZZ, Wu Z. 2004. The intensification and shift of the annual North Atlantic Oscillation in a global warming scenario simulation. *Tellus Series A-Dynamic Meteorology and Oceanography* **56**: 112–124.

Hurrell JW. 1995. Decadal trends in the North Atlantic Oscillation and relationships to regional temperature and precipitation. *Science* **269**: 676–679.

Hurrell JW, Hoerling MP, Phillips AS, Xu T. 2004. Twentieth century North Atlantic climate change. Part 1: assessing determinism. *Climate Dynamics* **23**(3–4): 371–389.

Huth R. 1997. Continental-scale circulation in the UKHI GCM. *Journal of Climate* **10**: 1545–1561.

Huth R. 2000. A circulation classification scheme applicable in GCM studies. *Theoretical and Applied Climatology* **67**(1–2): 1–18.

IPCC. 2001. *Climate Change 2001: Synthesis Report. A Contribution of Working Groups I, II, and III to the Third Assessment Report of the Integovernmental Panel on Climate Change*, Watson RT, and the Core Writing Team (eds). Cambridge University Press: Cambridge, New York; 398.

Jenkinson AF, Collison FP. 1977. An initial climatology of gales over the North Sea, Synoptic Climatology Branch Memorandum 62: Meteorological Office, London.

Jones PD, Hulme M, Briffa KR. 1993. A comparison of Lamb circulation types with an objective classification scheme. *International Journal of Climatology* **13**: 655–663.

Jungclaus JH, Botzet M, Haak H, Keenylside N, Luo J-J, Latif M, Marotzke J, Mikolajewicz U, Roeckner E. 2006. Ocean circulation and tropical variability in the coupled model ECHAM5/MPI-OM. *Journal of Climate* **19**: 3952–3972.

Lamb HH. 1972. British isles weather types and a register of daily sequence of circulation patterns, 1861–1971. *Geophysical Memoir* **116**: 85, HMSO, London.

Latif M, Arpe K, Roeckner E. 2000. Oceanic control of decadal North Atlantic sea level pressure variability in winter. *Geophysical Research Letters* **27**: 727–730.

Copyright © 2008 Royal Meteorological Society

DOI: 10.1002/joc

Loptien U, Ruprecht E. 2005. Effect of synoptic systems on the variability of the North Atlantic Oscillation. *Monthly Weather Review* **133**: 2894–2904.

Marshall J, Kushnir Y, Batisti D, Chang P, Czaja R, Dicson R, Hurrell J, McCartney M, Saravanan R, Visbeck M. 2001. North Atlantic climate variability: phenomena, impacts and mechanisms. *Journal of Climatology* **21**: 1863–1898.

Marsland SJ, Haak H, Jungclaus JH, Latif M, Röske F. 2003. The Max-Planck-Institute global ocean/sea ice model with orthogonal curvilinear coordinates. *Ocean Modelling* **5**(2): 91–127.

McKendry IG, Stahl K, Moore RD. 2006. Synoptic sea-level pressure patterns generated by a general circulation model: comparison with the types derived from NCEP/NCAR re-analysis and implications for downscaling. *International Journal of Climatology* **26**: 1727–1736.

Osborn TJ, Briffa KR, Tett SFB, Jones PD, Trigo RM. 1999. Evaluation of the North Atlantic Oscillation as simulated by a coupled climate model. *Climate Dynamics* **15**: 685–702.

Post P, Truija V, Tuulik J. 2002. Circulation weather types and their influence on temperature and precipitation in Estonia. *Boreal Environmental Research* **7**: 281–289.

Raible CC. 2007. On the relation between extremes of midlatitude cyclones and the atmospheric circulation using ERA40. *Geophysical Research Letters* **34**: 1–6.

Raible CC, Blender R. 2004. Northern hemisphere midlatitutde cyclone variability in GCM simulations with different ocean representations. *Climate Dynamics* **22**: 239–248.

Raible CC, Stocker TF, Yoshimori M, Renold M, Beyerle U, Casty C, Luterbacher J. 2005. Northern hemispheric trends of pressure indices and atmospheric circulation patterns in observations, reconstructions, and coupled GCM simulations. *Journal of Climate* **18**: 3968–3982.

Roeckner E, Bäuml G, Bonaventura L, Brokopf R, Esch M, Giorgetta M, Hagemann S, Kirchner I, Kornblueh L, Manzini E, Rhodin A, Schlese U, Schulzweida U, Tompkins A. 2003. *The Atmospheric General Circulation Model ECHAM5*, Part 1, Model Description, Report 349. Max-Planck-Inst. For Meteorology: Hamburg, 127, [Available from Max Planck Institute for Meteorology, Bundesstr. 53, 20146, Hamburg, Germany].

Roeckner E, Brasseur GP, Giorgetta M, Jacob D, Jungclaus J, Reick C, Sillmann J. 2006b. Climate projections for the 21st century, Max Planck Institute for Meteorology, Internal Report, 28, [Available from Max Planck Institute for Meteorology, Bundesstr. 53, 20146, Hamburg, Germany].

Roeckner E, Brokopf R, Esch M, Giorgetta M, Hagemann S, Kornblueh L, Manzini E, Schlese U, Schulzweida U. 2006a. Sensitivity of simulated climate to horizontal and vertical resolution in the ECHAM5 atmosphere model. *Journal of Climate* **19**: 3771–3791.

Rogers JC. 1997. North Atlantic storm track variability and its association to the North Atlantic Oscillation and climate variability of Northern Europe. *Journal of Climate* **10**: 1635–1647.

Schar C, Vidale PL, Luthi D, Frei C, Haberli C, Liniger MA, Appenzeller C. 2004. The role of increasing temperature variability in European summer heatwaves. *Nature* **427**: 332–336.

Scherrer SC, Croci-Maspoli M, Schwierz C, Appenzeller C. 2006. Two-dimensional indices of atmospheric blocking and their statistical relationship with winter climate patterns in the Euro-Atlantic region. *International Journal of Climatology* **26**(2): 233–249.

Schwierz C, Appenzeller C, Davies HC, Liniger MA, Muller W, Stocker TF, Yoshimori M. 2006. Challenges posed by and approaches to the study of seasonal-to-decadal climate variability. *Climatic Change* **79**(1–2): 31–63.

Serreze MC, Carse F, Barry RG, Rogers JC. 1997. Icelandic low cyclone activity: climatological features, linkages with the NAO, and relationships with recent changes in the Northern Hemisphere circulation. *Journal of Climate* **10**: 453–464.

Sickmöller M, Blender R, Fraedrich K. 2000. Observed winter cyclone tracks in the Northern Hemisphere in re-analyzed ECMWF-data. *Quaternary Journal of the Royal Meteorology Society* **126**: 591–620.

Tibaldi S. 1993. Low frequency variability and blocking as diagnostic tools for global change models. In *Prediction of Interannual Climate Variations. NATO-ASI Series 1*, Vol. 6, Shukla J (ed.). Springer-Verlag, Berlin Heidelberg: New York; 173–182.

Trigo RM, Dacamara CC. 2000. Circulation weather types and their influence on the precipitation regime in Portugal. *International Journal of Climatology* **20**: 1559–1581.

Trigo RM, Osborn TJ, Corte-Real JM. 2002. The North Atlantic Oscillation influence on Europe: climate impacts and associated physical mechanisms. *Climate Research* **20**: 91–17.

Trigo RM, Trigo IF, DaCamara CC, Osborn TJ. 2004. Climate impact of the European winter blocking episodes from the NCEP/NCAR Reanalyses. *Climate Dynamics* **23**: 17–28.

Ulbrich U, Christoph M. 1999. A shift in the NAO and increasing storm track activity over Europe due to anthropogenic greenhouse gas. *Climate Dynamics* **15**: 551–559.

Uppala SM, Allberg K, Simmons PW, Andrae AJ, Da Costa U, Bechtold V, Fiorino M, Gibson JK, Haseler J, Hernandez A, Kelly GA, Li X, Onogi K, Saarinen S, Sokka N, Allan RP, Andersson E, Arpe K, Balmaseda MA, Beljaars ACM, Van De Berg L, Bidlot J, Bormann N, Caires S, Chevallier F, Dethof A, Dragosavac M, Fisher M, Fuentes M, Hagemann S, H'olm E, Hoskins BJ, Isaksen L, Janssen PAEM, Jenne R, Mcnally AP, Mahfouf J-F, Morcrette J-J, Rayner NA, Saunders RW, Simon P, Sterl A, Trenberth KE, Untch A, Vasiljevic D, Viterbo P, Woollen J. 2005. The ERA-40 re-analysis. *Quarterly Journal of the Royal Meteorological Society* **131**: 2961–3012.

van Ulden AP, van Oldenborgh GJ. 2006. Large-scale atmospheric circulation biases and changes in global climate model simulations and their importance for climate change in Central Europe. *Atmospheric Chemistry and Physics* **6**: 863–881.

Verstraeten G, Poesen J, Demarée G, Salles C. 2006. Long-term (105 years) variability in rain erosivity as derived from 10-min rainfall depth data for Ukkel (Brussels, Belgium): Implications for assessing soil erosion rates. *Journal of Geophysical Research* **111**: 1–11.

Copyright © 2008 Royal Meteorological Society

DOI: 10.1002/joc